ELSEVIER

Biophysical Chemistry 97 (2002) 55–72

Biophysical Chemistry

www.elsevier.com/locate/bpc

Interaction of the IP_3-Ca^{2+} and the FGF-MAPK signaling pathways in the *Xenopus laevis* embryo: a qualitative approach to the mesodermal induction problem

José Díaz[a,b,*], Gerold Baier[a], Gustavo Martínez-Mekler[b], Nina Pastor[a]

[a]*Facultad de Ciencias, Universidad Autónoma del Estado de Morelos, Av. Universidad 1001, Col. Chamilpa, Cuernavaca, Morelos, Mexico C.P. 62210*

[b]*Centro de Ciencias Físicas, Universidad Nacional Autónoma de México, Apdo. Postal 48-3, Ave. Universidad S/N, Chamilpa, Cuernavaca, Morelos, Mexico*

Received 19 December 2001; received in revised form 12 February 2002; accepted 12 February 2002

Abstract

In this work we propose that the animal–vegetal gradient spatial distribution of the IP_3 receptors observed in the *Xenopus* embryo can effect a uniform FGF inducting input signal, allowing for different modes of transcription of the Xbra gene, producing the differentiation of the cells of the marginal zone. We analyze this hypothesis with a model for the interaction of the calcium signaling system with the MAPK cascade during the FGF mesodermal induction process, consisting of five non-linear coupled differential equations. A numerical treatment of a one- and two-cell system shows that the calcium flux between cells enhances the Raf activity levels, leading to oscillatory behavior. This qualitative result may be of consequence for the expression of the ventralizing characteristics of the FGF inducting signal.

Keywords: Fibroblast growth factor (FGF); Calcium spikes; Mitogen-activated protein kinase (MAPK) cascade; Mesodermal induction; Inositol 1,4,5-trisphosphate (IP_3) receptor; Mathematical model; Non-linear dynamics; Synchronization of cells

1. Introduction

The mesoderm is the set of embryonic cells that has the information to build the notochord, heart, blood and other related tissues of the organism. The differentiation of these cells is the process known as mesodermal induction. It initiates at the mid-blastula transition (MBT) stage of the *Xenopus* embryo, under the influence of members of the transforming growth factor family (TGFβ) and the fibroblast growth factor (FGF). The experimental records at this stage show that there is an intense periodic production of calcium signals from a region close to the equatorial zone [1]. In this work, we looked into the role that these periodic calcium signals might have on the mesodermal induction process, in particular their influence on the dynamics of the MAPK signaling pathway activated by FGF.

*Corresponding author. Tel.: +52-777-3297020; fax: +52-777-3297940.

E-mail address: jdiaz@fis.unam.mx (J. Díaz).

0301-4622/02/$ - see front matter
PII: S0301-4622(02)00039-X

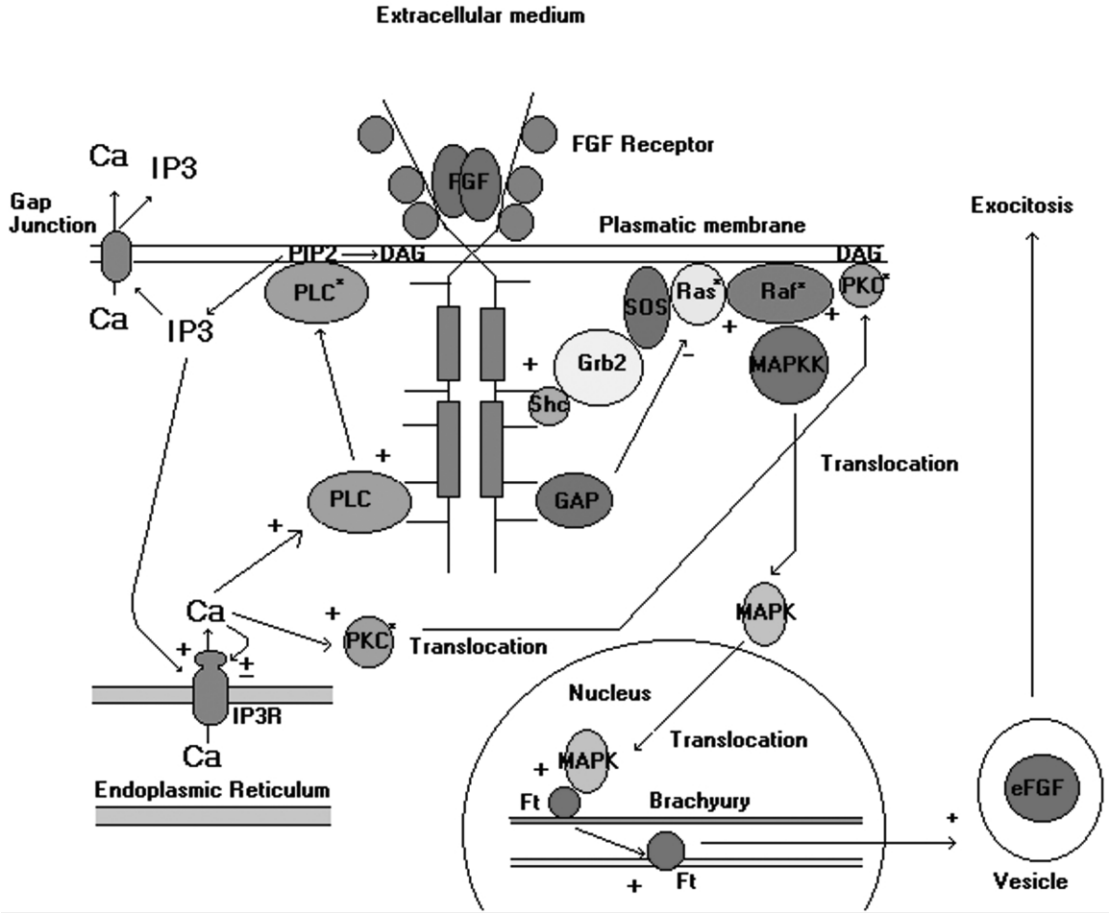

Fig. 1. The FGF receptor is linked to the Ca^{2+} and MAPK signaling systems. The symbol (+) indicates an activating process and the symbol (−) indicates an inactivating process.

Basic FGF (bFGF) and *Xenopus* eFGF (XeFGF) are proteins that act as one of the inductors of mesodermal differentiation. They appear to be uniformly distributed in the embryo at the beginning of the induction process [2]. Both FGF isoforms act through the MAPK intracellular signaling pathway and co activate, together with activin, the Brachyury gene of *Xenopus* (Xbra) [2–6]. When the Xbra gene is switched on, the embryo begins the synthesis of the zygotic XeFGF [2,7,8]. FGF isoforms also activate the IP_3-Ca^{2+} signaling system through the phosphorylation of phospholipase Cγ1 (PLCγ1). Fig. 1 shows the molecules that participate in the transmission of the signal from the external cell surface to the nucleus.

Although some experimental facts indicate that PLCγ1 activation does not have a direct role in the mesodermal induction process [9], other experiments show that the blocking of the IP_3 receptor (IP_3R) with monoclonal antibodies induces dorsal differentiation [10]. Furthermore, it has been found that the IP_3 receptors are uniformly distributed along the dorso–ventral axis of the embryo; however, they are distributed along a gradient in the animal–vegetal axis direction [11]. Most of these receptors are located at the perinuclear zone of the animal pole cells.

This gradient distribution of the IP_3R might be a structural property of the system, with consequences for the mesodermal induction process. It is an intriguing fact that the activation of the FGFR triggers three different signaling pathways: MAPK cascade, PI3Ks and IP_3-Ca^{2+}. The latter two pathways converge in the MAPK cascade [12,13]. The activation of the Xbra gene is directly related to the action of FGF through the MAPK cascade [8]. The calcium signal may, therefore, play an important role in the spatio-temporal features of the induction signal. We propose that the spatial distribution of the IP_3R affects the uniform FGF input signal, allowing for different modes of transcription of the Xbra gene, producing the differentiation of the cells of the marginal zone, even if all the embryonic cells were submerged in the same FGF external concentration.

In this paper, we analyze the above hypothesis with a mesodermal induction process model, consisting of five coupled non-linear differential equations. These equations describe the kinetics of: (a) activation of the FGFR on the cellular surface; (b) activation of Raf; (c) activation of PLC; (d) the free calcium ion concentration in the cytoplasm; and (e) the calcium concentration in the endoplasmic reticulum (ER) stores.

We first focus on the qualitative behavior of the model in a one-cell system by means of numerical integration, and then extend the investigation to a coupled two-cell system subject to a non-uniform distribution of IP_3R, in the presence of a uniform concentration of FGF. This analysis allows us to study the influence of the calcium dynamics resulting from the non-uniform IP_3R distribution on the temporal pattern of the Xbra gene expression.

2. The model

2.1. One-cell kinetic model for the mesodermal induction process by FGF

The qualitative model of the interaction of the calcium and MAPK signaling systems is based on the diagram in Fig. 1.

The FGF cellular surface receptors (FGFR) have a high affinity for their ligand ($K_d = 10^{-9}$–10^{-12} M) [14]. When FGF binds to its receptor, a self-phosphorylated dimeric complex with tyrosine kinase activity is formed [15,16]. In its simplest form, the formation of the agonist–receptor dimeric complex (C) is a two-step process: (1) one molecule of FGF binds to one cell-surface receptor FGFR and forms a F–FGFR complex; (2) the F–FGFR complex binds to another one, in the presence of heparan sulfate proteoglycan, to form a dimeric complex, which is activated by self-phosphorylation. If we denote concentration of the F–FGFR complex by T and that of the activated dimeric complex by C, the differential equations for this two-step process are:

$$\frac{dT}{dt} = k_1(FGF^e - T)(R - T) - k_2 T \quad (1)$$

$$\frac{dC}{dt} = k_3 T^2 - k_4 C \quad (2)$$

where FGF^e is the total concentration of the agonist in the external medium and R is the total amount of FGFR on the cell surface. The values of k_1, k_2, k_3 and k_4 are 4.76 $\mu M^{-1}\ s^{-1}$, 0.0008 s^{-1}, 6.25 $\mu M^{-1}\ s^{-1}$ and 0.001 s^{-1}, respectively [17]. Under steady state-conditions, from Eq. (1) we find:

$$T^{est} = \frac{\gamma}{2} - \frac{\sqrt{\gamma^2 - 4FGF^e R}}{2} \quad (3)$$

where $\gamma = FGF^e + R + \frac{k_2}{k_1}$.

Susbstituing Eq. (3) into Eq. (2), we finally find:

$$\frac{dC}{dt} = k_3 (T^{est})^2 - k_4 C \quad (4)$$

Previous work determined that the number of FGF receptors on the surface of Balb/c3T3 cells is approximately 15 000 receptors per cell [17]. Since we do not know the number of FGFR for *Xenopus* blastomeres, we analyzed the influence of the value of R on the one-cell calcium dynamics in order to set an interval of values for this parameter for which an oscillatory calcium response arises. This analysis is presented later.

As shown in Fig. 1, the dimeric complex phosphorylates a group of three intracellular proteins:

the Sh2–Sh3 adapter Shc-Grb2, phospholipase Cγ1 (PLCγ1) and the GTPase-activating protein (GAP) [5]. The Grb2- and GAP-activated proteins form a negative feedback loop that modulates the amount of activated Ras in the cell cytoplasm [18].

We assume in our model that the temporal behavior of the overall negative feedback loop is a balance between the rate of formation of Shc-Grb_2 and the rate of activation of the GAP molecule, both of which are related to C via Michaelis–Menten kinetics [19]. This balance determines the rate of activation of Ras. The balance equation for the total amount of activated Ras, denoted by Ras^*, can then be written as:

$$\frac{\mathrm{d}\ Ras^*}{\mathrm{d}t} = \frac{k_5 C}{C+k_6}(Ras_T - Ras^*) - \frac{k_7 C}{C+k_8} Ras^* \qquad (5)$$

The values of the constants are: $k_5 = 0.003\ s^{-1}$; $k_6 = 0.0166\ \mu M$; $k_7 = 0.08\ s^{-1}$; and $k_8 = 0.013\ \mu M$. The total amount of Ras (denoted by Ras_T) was set to 0.1 μM [19,20].

From the Grb2–GAP loop, the signal travels through a cascade of MAP kinases. The first of these is Raf1, which is a MAP kinase-kinase-kinase (MAPKKK). Raf1 is translocated under the influence of phosphatidic acid to the inner surface of the plasma membrane [21], where it acquires its serine/threonine kinase function (denoted by Raf^*) in the presence of activated Ras.

As shown in Fig. 1, two feedback loops converge at the Raf level. A positive feedback loop is due to the action of PKC^* on the Raf molecule. The rate of this process is directly determined by the calcium cytosolic concentration Ca, and we model it with Michaelis–Menten kinetics [19]. Raf^* is in turn deactivated by its own phosphatase.

The overall rate of formation of Raf^* is then:

$$\frac{\mathrm{d}\ Raf^*}{\mathrm{d}t} = \left(k_9 Ras^* + \frac{k_{10} Ca}{Ca + k_{11}}\right) \times (Raf_T - Raf^*) - \frac{k_{12} Raf^*}{Raf^* + k_{13}} \qquad (6)$$

The parameter values we used are: $k_9 = 0.025\ \mu m^{-1}\ s^{-1}$; $k_{10} = 0.005\ s^{-1}$; $k_{11} = 4\ \mu M$; $k_{12} = 0.002\ \mu M\ s^{-1}$; and $k_{13} = 0.008\ \mu M$. The total amount of Raf_T was set to 0.3 μM [19,20].

Under steady-state conditions, from Eq. (5) we find:

$$Ras^* = \frac{Ras_T}{1 + \dfrac{k_7(C+k_6)}{k_5(C+k_8)}} \qquad (7)$$

Substituting Eq. (7) into Eq. (6), we obtain a steady-state balance equation for activated Raf:

$$\frac{\mathrm{d}\ Raf^*}{\mathrm{d}t} = \left(\frac{k_9 Ras_T}{1 + \dfrac{k_7(C+k_6)}{k_5(C+k_8)}} + \frac{k_{10} Ca}{Ca + k_{11}}\right) \times (Raf_T - Raf^*) - \frac{k_{12} Raf^*}{Raf^* + k_{13}} \qquad (8)$$

Raf^* acts specifically on a MAP-kinase-kinase (MAPKK), either *Xenopus* MEK1 or MEK2. Each of these kinases phosphorylates the tyrosine and threonine residues of a MAP-kinase (MAPK) in a specific way. In *Xenopus*, the MAPKs could be either ERK1 or ERK2, which are translocated to the nucleus, where they act on a transcription factor that activates the Xbra gene [8,22].

We consider that activated MAPKK and MAPK rapidly reach a quasi-stationary state with respect to the concentration of Raf^*, and hence we did not explicitly model the phosphorylation process of the kinases downstream of Raf.

The phosphorylated molecule of PLCγ1 (denoted by PLC^*) activates the synthesis of IP_3 from inositol-4,5-bisphosphate (PIP_2) of the plasma membrane. The IP_3 triggers an intense periodic calcium efflux from the endoplasmic reticulum (ER) stores. In this work, we consider that IP_3 rapidly reaches a quasi-stationary state with respect to the PLC* concentration, and that the behavior of this positive feedback loop is completely determined by the temporal behavior of the PLC^* and calcium concentrations [23]

The calcium spikes produced by IP_3 influence the signal that travels through the MAPK pathway, because a high level of calcium in the cytoplasm

activates protein kinase C (PKC). The activated PKC (denoted by PKC^*) acts on the CR3 domain of the Raf molecule, increasing its MAPKKK activity [24].

The calcium ion also acts on PLC [25], closing a positive feedback loop in which the rise in the level of PLC^* increases the IP_3 concentration, and the latter increases calcium efflux from the ER. This mechanism allows for sustained oscillations of the free calcium concentration in the cytoplasm; however, it is not clear which isoform of PLC is activated by calcium, since PLCδ, PLCγ1 and PLCβ can all be possible targets of the calcium ion [26]. The PLCβ and PLCγ1 isoforms can act in concert, each contributing to a specific aspect of the calcium response [27]. We do not have information about the presence of PLCδ in the *Xenopus* embryo.

The rate of activation of PLCγ1 by the dimeric complex can be modeled by Michaelis–Menten-type kinetics [19] if we consider that the PLC activation occurs in a two-step process described by the following reactions:

$$\mathrm{PLC} + C \leftrightarrow \mathrm{PLC^{tr}}$$

$$\mathrm{PLC^{tr}} \rightarrow \mathrm{PLC^*} + C$$

with the kinetic equations:

$$\frac{\mathrm{d}\ \mathrm{PLC^{tr}}}{\mathrm{d}t} = k_{\mathrm{I}}\mathrm{PLC}\cdot C - k_{-\mathrm{I}}\mathrm{PLC^{tr}} \tag{9}$$

$$\frac{\mathrm{d}\ \mathrm{PLC^*}}{\mathrm{d}t} = k_{\mathrm{II}}\mathrm{PLC^{tr}} \tag{10}$$

If the first step rapidly reaches the steady state, from Eq. (9) we can obtain an expression for PLC^{tr}, considering the fact that $PLC = PLC_{Total} - PLC^{tr}$. This relation can be substituted into Eq. (10) to lead to an equation for the velocity of activation of PLC by the dimeric complex (C):

$$\frac{\mathrm{d}\ \mathrm{PLC^*}}{\mathrm{d}t} \approx \frac{k_{14}C}{C + k_{15}} \tag{11}$$

Although we do not know which isoform of the PLC is activated by the calcium ion [25], we added a term for the activation of this phospholipase, in which its rate of activation by calcium is proportional to the cytosolic Ca^{2+} concentration.

Finally, the PLC^* is inactivated with a rate proportional to its own concentration.

The balance equation for the overall rate of PLC^* activation is then:

$$\frac{\mathrm{d}\ \mathrm{PLC^*}}{\mathrm{d}t} = \frac{k_{14}C}{C + k_{15}} + k_{16}\mathrm{Ca} - k_{17}\mathrm{PLC^*} \tag{12}$$

The parameter values $k_{14} = 3.5\ \mu\mathrm{M\ s^{-1}}$ and $k_{15} = 0.033\ \mu\mathrm{M}$ were taken from the literature [20]. The values of the other parameters, $k_{16} = 0.08\ \mathrm{s^{-1}}$ and $k_{17} = 1.7\ \mathrm{s^{-1}}$, were chosen so that the steady concentration of PLC^* does not exceed 0.3 μM. The balance between the values of k_{11} and k_{14} sets the amplitude of the spikes if the other parameters of the model are held at a constant value.

For the purpose of modeling the oscillations in the intracellular calcium concentration, it is not necessary to model the IP_3 receptor kinetics, because they are primarily due to the balance between the positive PLC feedback loop and the calcium damping mechanisms [23]. The high levels of calcium are periodically damped by the action of the ER calcium pumps, which can be modeled by saturation dynamics with a Hill coefficient equal to two. We assume that the amplitude of the spikes is also influenced by the release of calcium from a calcium-sensitive store dependent on the cytoplasm calcium concentration and on the ER calcium concentration [1,25].

In *Xenopus,* there is also a continuous calcium influx from the extracellular space through L-type calcium channels. These channels are dihydropyridine-sensitive and cause an increase in the cytosolic calcium concentration. They are modulated by PKC^* in the presence of diacylglycerol (DAG) in the plasma membrane [28,1]. This influx or leak is taken into account in order to obtain a more detailed balance equation for the free cytosolic calcium [23,29]. We assume that it is proportional to the PLC^* concentration which triggers the production of DAG.

In our model the calcium ionic current from the ER (I_{Ca}) depends on the number of IP_3 receptors

(N), on the probability that the receptor is open at time t (p_o) and on the unitary current through the channel (i):

$$I_{Ca} = N\ p_o\ i \tag{13}$$

The probability p_o is a function of the cytosolic calcium concentration. The probability of being open is a bell-shaped function of the cytosolic calcium concentration [30]; however, in some cases a hyperbolic function of the saturation kinetics-type has been proposed [29]. In our model we use the latter approach with a Hill coefficient equal to one, because the mechanism that produces calcium oscillations is mainly the initial, fast activation of the IP_3R and its subsequent slow inactivation [29]. Furthermore, this probability also depends on PLC^* because the IP_3 concentration is in a quasi-steady state with respect to it. Thus, the expression for the p_o term is:

$$p_o = A\cdot\left(\frac{Ca}{Ca + k_{19}}\right)\cdot PLC^* \tag{14}$$

where A is a normalization factor necessary to transform p_o into a probability function. That is:

$$A\int_{-\infty}^{\infty}\int_{-\infty}^{\infty}\left(\frac{Ca}{Ca + k_{19}}\right)PLC^*\cdot d\,Ca\cdot d\,PLC^* = 1 \tag{15}$$

If all the cells were exposed to the same agonist concentration and had the same number of IP_3R, then A would be a constant.

The unitary current term can be approximated by the equation:

$$i = 2\times 10^6\cdot(kFV)\cdot CaS \tag{16}$$

where F is the Faraday constant (96 500 C mol^{-1}), V is the volume of the cell in l, CaS is the calcium concentration in the ER measured in μM and κ is a rate constant in s^{-1}.

The resulting expression for I_{Ca} is:

$$I_{Ca} = 2\times 10^6\cdot(kFUNA)\cdot\left(\frac{Ca}{Ca + k_{19}}\right)PLC^*\cdot CaS \tag{17}$$

which finally leads to an equation for the increase in cytosolic calcium resulting from the ER calcium stores (Ca_{ER}):

$$\frac{d\ Ca_{ER}}{dt} = NA\kappa\cdot\left(\frac{Ca}{Ca + k_{19}}\right)\cdot PLC^*\cdot CaS \tag{18}$$

The overall rate of change of the free cytosolic calcium concentration is a balance among the influx of calcium from the ER, the influx of calcium from the L-type Ca channels, the calcium pumped by the ER pumps, the release of calcium through the calcium-sensitive store of the ER and the calcium buffered by PLC and PKC during their activation:

$$\frac{d\ Ca}{dt} = \frac{k_{18}CaS\cdot PLC^*\cdot Ca}{Ca + k_{19}} + k_{20}PLC^* - \frac{k_{21}Ca^2}{Ca^2 + k_{22}} + \frac{k_{23}Ca^2Cas}{Ca^2 + k_{24}} - k_{16}Ca - \frac{k_{10}Ca}{Ca + k_{11}} \tag{19}$$

where k_{18} is a control parameter that determines the intensity of the calcium flux from the ER and is defined from Eq. (18) as:

$$k_{18} = NA\kappa \tag{20}$$

The values of the other parameters are: k_{19} = 0.33 μM; k_{20} = 1.5 s^{-1}; k_{21} = 30 μM s^{-1}; k_{22} = 0.512 μM^2; k_{23} = 2.5 s^{-1}; and k_{24} = 0.512 μM^2 [23,25,29].

Finally, the rate of change of the calcium concentration of the ER stores is:

$$\frac{d\ CaS}{dt} = -\frac{k_{18}CaS\cdot PLC^*\cdot Ca}{Ca + k_{19}} + \frac{k_{21}Ca^2}{Ca^2 + k_{22}} - \frac{k_{23}Ca^2CaS}{Ca^2 + k_{24}} \tag{21}$$

2.1.1. Spatial and temporal scales of the process

The set of equations Eq. (4), Eq. (8), Eq. (12), Eq. (19) and Eq. (21) describes the temporal response of one cell to FGF under steady-state conditions. The time interval for the computer simulation of the model ranges from the beginning

of the MBT stage, at the end of the 12th mitotic division, to the beginning of the 13th mitotic division.

Up to the 12th mitotic division, cleavage is synchronous, but at the 13th mitotic division cleavage becomes asynchronous: the mitotic division is faster for the animal pole cells than for the vegetal pole cells. Consequently, from the 13th mitotic division on, the concentration of the signaling molecules varies drastically and non-uniformly in both poles and the model assumptions cannot be properly extended to investigate the temporal behavior of all the embryo cells. To avoid this problem, we limited the simulation of the model to a time interval of 1200 s, which approximately corresponds to the time interval between both mitotic division periods.

We assume that the blastomeres have an average cytosolic volume of 0.128 nl and an average diameter of 62.67 μm. All concentrations are referred to these values. We do not take into account the vesicular traffic of FGF and its receptor, nor the translocation process of the PLC^*, Raf^* and PKC^* molecules to the inner surface of the plasma membrane.

Numerical analysis of the model was performed with the Euler Predictor–Corrector Method, with a time step of 0.04. The initial conditions used are: $C = Raf^* = PLC^* = 0$; $Ca = 0.01$ μM and $CaS = 12$ μM.

2.2. Two-cell kinetic model for the mesodermal induction process by FGF

As a first step towards our understanding of how the animal–vegetal gradient of IP_3 receptors affects the kinetic properties of the calcium and MAPK signaling pathways, we simulated the interaction of two cells with a different amount of IP_3 receptors. It is not necessary to modify the core of the model for one cell, because only the calcium ion can diffuse across cells.

The modified equations are:

$$\frac{dC_j}{dt} = k_3(T^{est})^2 - k_4 C_j$$

$$\frac{dRaf_j^*}{dt} = \left(\frac{k_9 Ras_T}{1 + \dfrac{k_7(C_j + k_6)}{k_5(C_j + k_8)}} + \frac{k_{10} Ca_j}{Ca_j + k_{11}} \right) \times (Raf_T - Raf_j^*) - \frac{k_{12} Raf_j^*}{Raf_j^* + k_{13}}$$

$$\frac{d\ PLC_j^*}{dt} = \frac{k_{14} C_j}{C_j + k_{15}} + k_{16} Ca_j - k_{17} PLC_j^*$$

$$\frac{d\ Ca_j}{dt} = f_j \frac{k_{18}^{(1)} Ca_j CaS_j PLC_j^*}{Ca_j + k_{19}} + k_{20} PLC_j^* - \frac{k_{23} Ca_j^2 (12 - CaS_j)}{Ca_j^2 + k_{24}} - k_{16} Ca_j - \frac{k_{10} Ca_j}{Ca_j + k_{11}} + (-1)^j D_{Ca}(Ca_1 - Ca_2)$$

$$\frac{d\ Cas_j}{dt} = -f_j \frac{k_{18}^{(1)} Ca_j CaS_j PLC_j^*}{Ca_j + k_{19}} + \frac{k_{23} Ca_j^2 (12 - CaS_j)}{Ca_j^2 + k_{24}} \quad (22)$$

where $j = 1,2$ is the number of the cell and $f_j = \dfrac{k_{18}^{(j)}}{k_{18}^{(1)}}$ is a measure of the relative number of receptors of the jth cell with respect to cell 1, which incorporates information on the ER receptor inhomogeneity. Since the parameter k_{18} is given in terms of the number of IP_3 receptors (N) and the normalization factor A by the expression $k_{18} = NA\kappa$, its value in cell j is related to that in cell 1 by:

$$k_{18}^{(j)} = \frac{N_j A_j}{N_1 A_1} k_{18}^{(1)} \quad (23)$$

and consequently $f_j = \dfrac{N_j A_j}{N_1 A_1}$.

We solved the model numerically as in the one-cell case. In the absence of quantitative data for the amount of receptors in the vegetal pole [19], we used different values of f_2, from 0.5 to 0.7, in order to simulate the transition from a sharp to a soft receptor gradient. D_{Ca} varied from 0 (no coupling) to 0.015 (strong coupling). The parameters $k_{18}^{(1)}$ and R were set to 20 $\mu M^{-1}\ s^{-1}$ and 0.0006 μM, respectively, and the concentration of FGF to 0.25 nM.

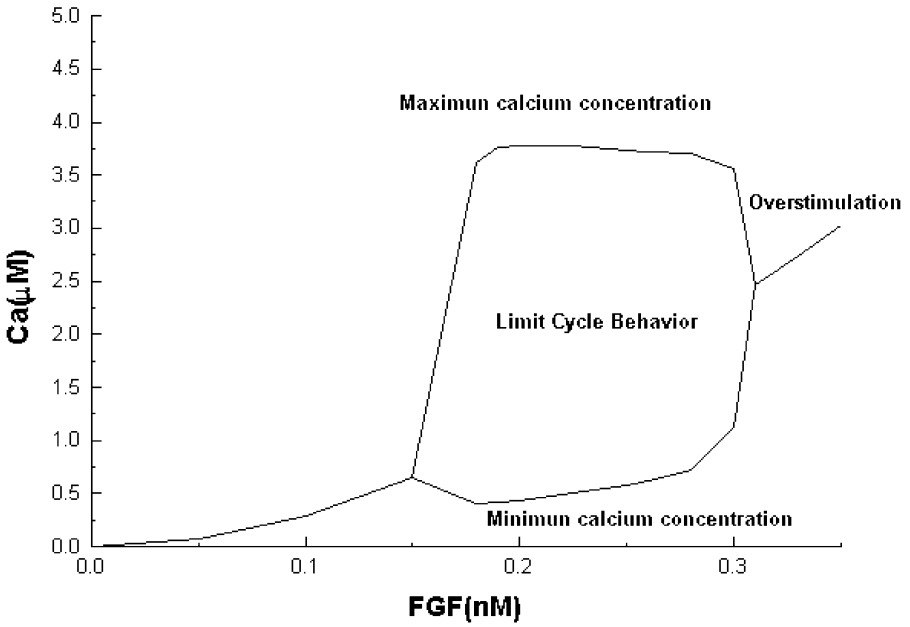

Fig. 2. Bifurcation diagram of the effect of the external FGF concentration on the intracellular calcium dynamics. The parameters k_{18} and R were held at constant values of 20 $\mu M^{-1}\ s^{-1}$ and 0.6 nM, respectively.

The initial conditions used were: $C_j = Raf_j^* = PLC_j^* = 0$; $Ca_j = 0.01$ μM and $CaS_j = 12$ μM.

3. Results

3.1. Calcium spikes

The calcium dynamics predicted by the model is strongly FGF-dependent. Fig. 2 shows the dependence of the amplitude of the calcium spikes on the external FGF concentration for a k_{18} value of 20 $\mu M^{-1}\ s^{-1}$. When the agonist concentration is below 0.18 nM, the cytosolic free calcium concentration increases with the FGF concentration, but the system does not reach the threshold concentration needed to start oscillatory dynamics. At a threshold FGF concentration of 0.18 nM, calcium spikes arise and their amplitude varies very little in the interval of agonist concentration between 0.18 and 0.28 nM. This is a very important feature of the model, because it allows a frequency encoding process with great accuracy (see Fig. 2). In the interval between 0.28 and 0.35 nM, the amplitude of the spikes decreases while the frequency increases, and for an agonist concentration above 0.35 nM, the oscillations cease but the free calcium concentration remains at a high cytosolic level, i.e. the system is over-stimulated [23].

The oscillatory dynamics of the system is strongly dependent on the value of the parameter k_{18}, which links the activation process of the PLC molecules with the calcium influx from the ER stores through the IP_3 receptors. Fig. 3a shows a bifurcation diagram for the parameter k_{18} at a FGF concentration of 0.25 nM. The calcium spikes arise at a threshold value of 11 $\mu M^{-1}\ s^{-1}$ and their amplitude becomes approximately constant in the interval between 15 and 60 $\mu M^{-1}\ s^{-1}$. For k_{18} values between 60 and 110 $\mu M^{-1}\ s^{-1}$ the amplitude of the spikes continuously decreases until a k_{18} value of 75 $\mu M^{-1}\ s^{-1}$, above which the system reaches an unstable steady state. From these results, we chose a k_{18} value of 20 $\mu M^{-1}\ s^{-1}$ as the standard value for the model, because the calcium spikes obtained for this value have the amplitude required to approximately fit with the experimental records [1].

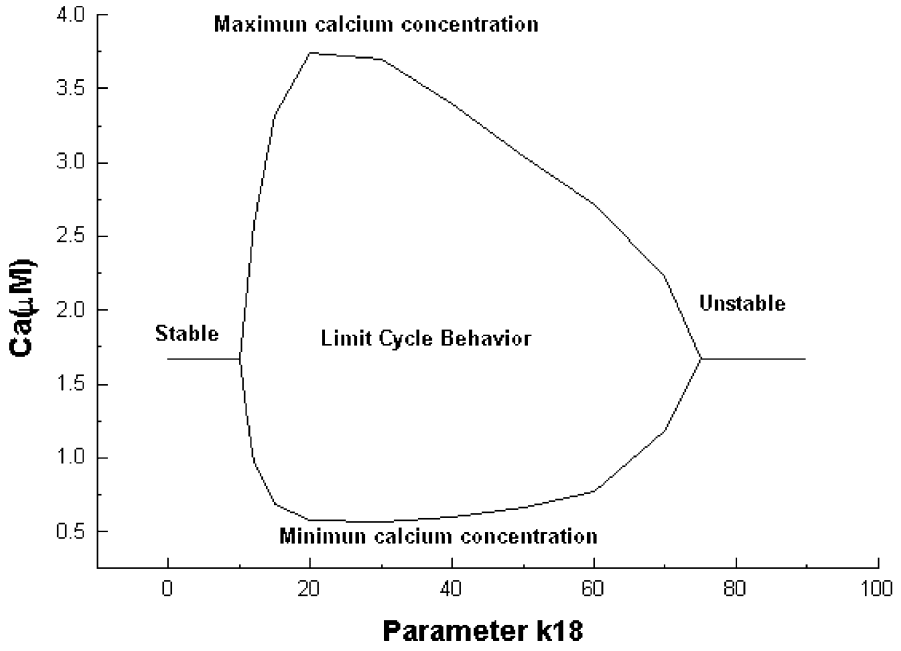

(a)

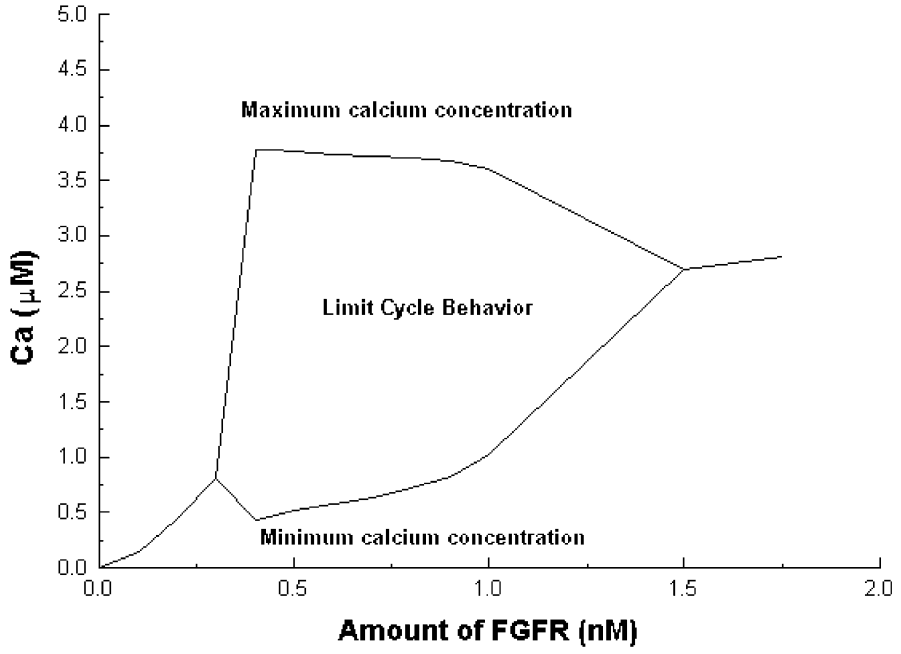

(b)

Fig. 3. (a) Bifurcation diagram for the parameter k_{18}. The FGF concentration used in this simulation was 0.25 nM and the parameter R was held at a value of 0.6 nM. (b) Bifurcation diagram for the parameter R. The FGF concentration used in this simulation was 0.25 nM and the parameter k_{18} was held at a value of 20 $\mu M^{-1}\ s^{-1}$.

An important problem of the model is its dependence on the number of FGF receptors at the cell surface. Since we do not have information from the literature about the exact value of this parameter, we explored the dependence of the calcium dynamics on it. The bifurcation diagram for R is shown in Fig. 3b. When the number of FGF receptors is approximately 31 000 (15 500 possible FGF dimeric complexes), calcium spikes arise in the system and their amplitude decreases above approximately 77 000 receptors (38 500 possible FGF dimeric complexes). The maximum amplitude of the spikes is reached when R has a value of close to 0.6 nM (46 000 FGF receptors). We chose this number of receptors as the standard value for the model.

The stimulation of the system by an agonist concentration above 0.2 nM drives the system to a stable limit cycle behavior, in which the variables PLC*, Ca and CaS show an oscillatory response. The oscillatory calcium-dependent dynamics of the system can hence be modeled considering the interplay between the activation of PLC by the FGFR dimeric complex, the influx of calcium from the ER, the activity of the Ca^{2+}-ATPases, calcium leakage through ionic channels and calcium buffering processes [23].

This limit cycle behavior induces a periodic modification of the basal level of activity of many molecules, such as PKC and other related Ca^{2+}-dependent molecules, as well as possible periodic variations in the number of Ca^{2+}-dependent translocation processes in the cytoplasm. All these factors can translate in turn the periodic changes in Ca^{2+} levels into periodic changes in the activity level of a great number of possible targets.

As PKC is the link between the PLC–Ca^{2+} signaling pathway and the FGF-MAPK pathway, the periodic changes in the number of PKC* molecules must be reflected in a periodic change in the number of Raf molecules activated by this kinase. The number of Raf molecules directly activated by the FGFR dimeric complex must be complemented with the Raf molecules activated by the PKC*. As consequence of this, the MAPK cascade acquires a limit cycle behavior; the whole signaling system oscillates with an amplitude and frequency that depend on the FGF concentration (Fig. 4).

These periodic changes in the levels of activity of the MAPK cascade must have an influence on the activity of the Xbra FGF-dependent transcription machinery. We do not have experimental information from the literature about this point, but the response of other genetic systems to the frequency of the calcium spikes opens this possibility [31].

3.2. Two cell system

In the early stages of *Xenopus* development, gap junctions electrically interconnect all the blastomeres. They remain open until cell differentiation begins. Cells of the same type remain interconnected, while the gap junctions that connected them to cells of another type close [32,33].

At stage 8 of development, these electric connections play a very important role during the mesodermal induction process. The experimental records obtained [1] show the presence of a calcium pacemaker placed at the prospective dorsal ectoderm domain. The intense calcium activity of this restricted area produces a set of calcium waves that propagate all over the embryo surface through the gap junctions. We suggest that this periodic calcium activity is due in part to the action of the FGF on its receptors (Fig. 1). The experimental records obtained from different groups do not clearly establish the spatial distribution of FGF at the beginning of stage 8 in the embryo; hence, the non-existence of an animal–vegetal gradient of FGF concentration remains a possibility [2,3,7,34]. In this work, we adopt this last point of view by considering that there is no regional difference in the concentration of the FGF that bathes the blastomeres. We also consider that any regional differences in the calcium activity are due in part to the non-homogeneous spatial distribution of IP_3R [10,11].

The coupling between cells depends on the conducting properties of the gap junctions, and these in turn depend on the intracellular calcium concentration. Even though high stationary Ca^{2+} concentrations can block the gap junctions, brief Ca^{2+} transients can freely pass through them [35].

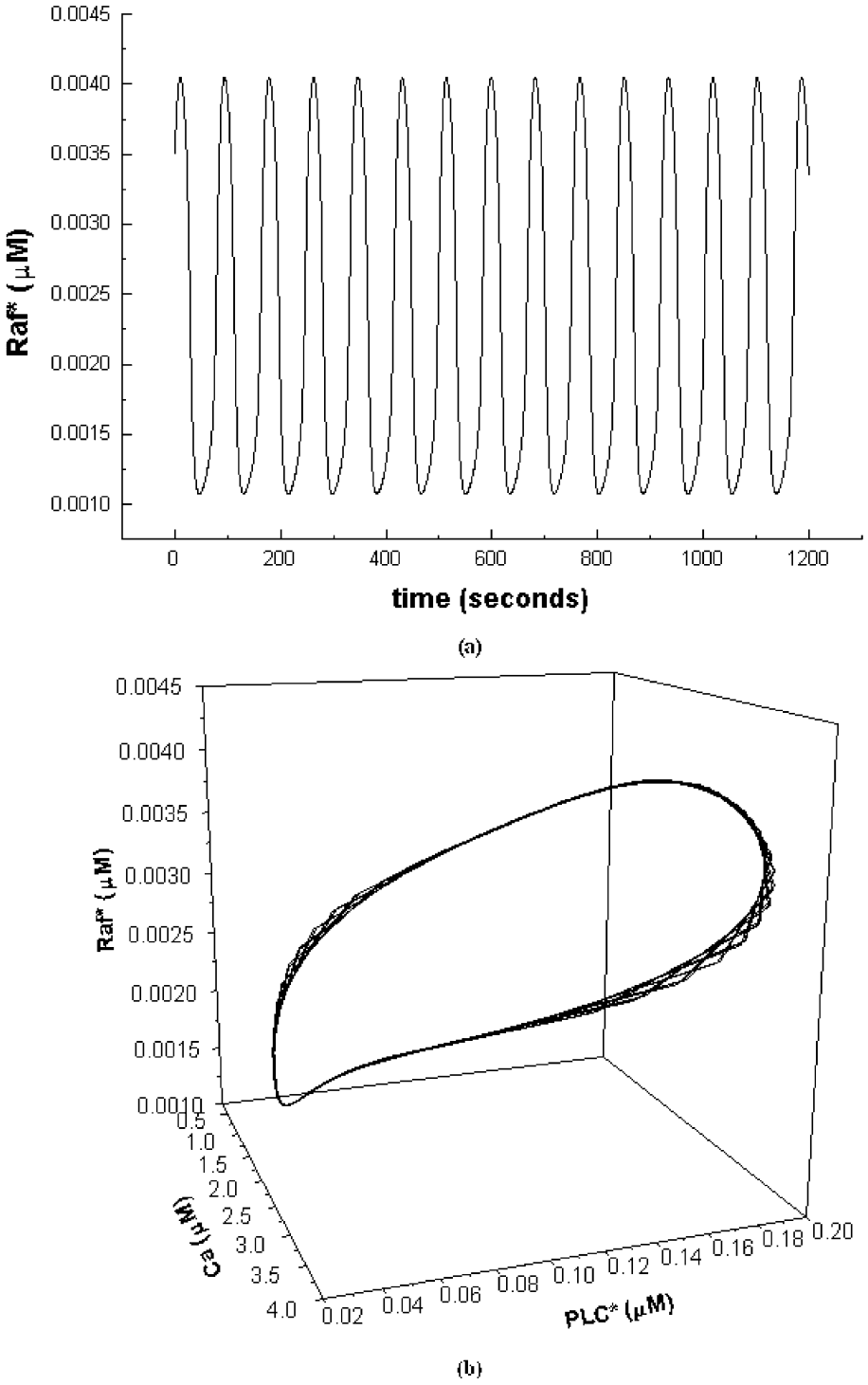

Fig. 4. (a) The calcium spikes induce periodic changes in the level of activation of Raf and (b) produce a stable limit cycle behavior of the system. The FGF concentration was 0.25 nM, the parameter k_{18} was held at a value of 20 $\mu M^{-1}\ s^{-1}$ and the parameter R at a value of 0.6 nM.

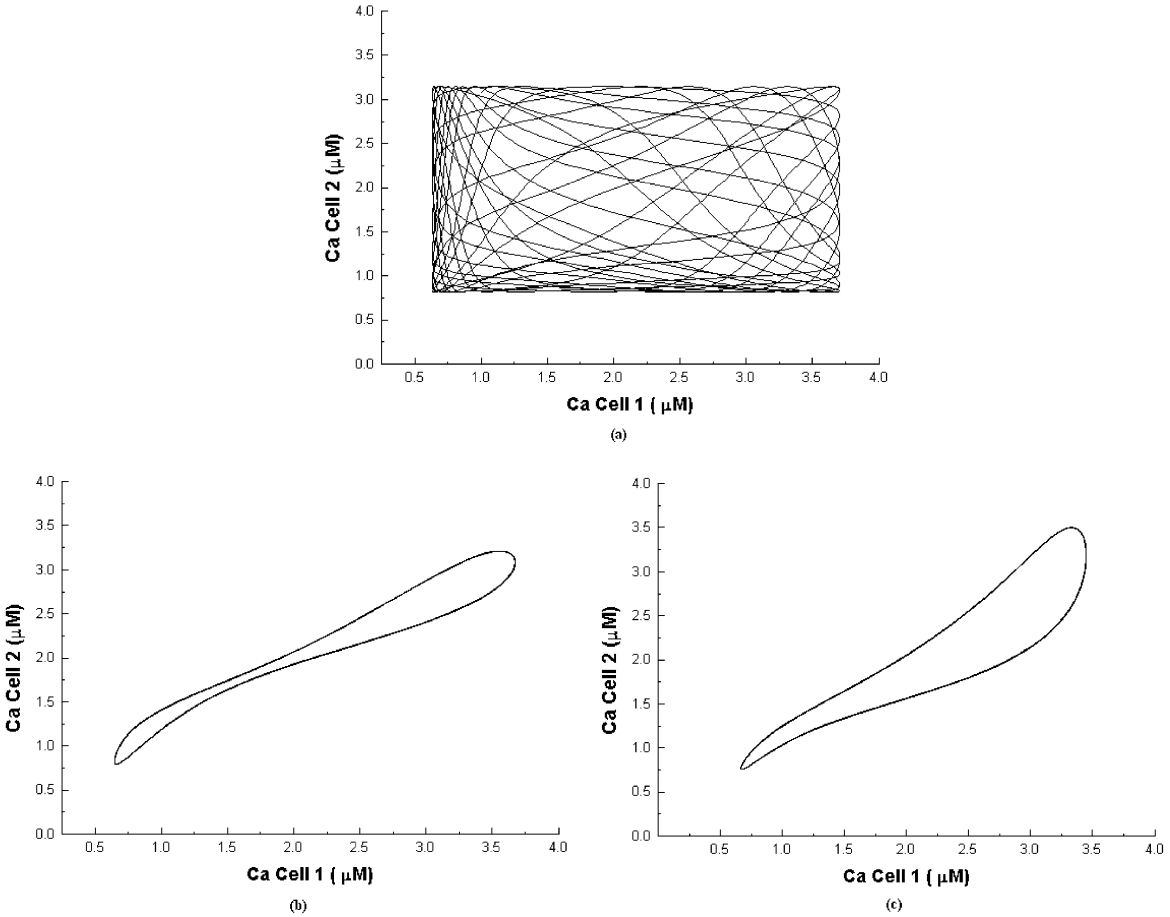

Fig. 5. Phase space plot for the calcium dynamics of: (a) two uncoupled cells; (b) soft coupling, $D_{Ca}=0.005\ s^{-1}$; and (c) strong coupling, $D_{Ca}=0.015\ s^{-1}$. In all panels, both cells were subjected to 0.25 nM of FGF. The parameters values used were: $f_2=0.7$ and $k_{18}^1=20\ \mu M^{-1}\ s^{-1}$.

In our model the coupling between cells is determined by the value of a coupling coefficient D_{Ca}. The average diameter of the cells is 62.67 μm, and thus a D_{Ca} value of 0.005 s^{-1} means that the gap-junctional calcium permeability is 0.3134 μm s^{-1} in the absence of buffering. In a similar way, a D_{Ca} value of 0.015 s^{-1} means that the gap-junctional calcium permeability is 0.94 μm s^{-1}.

Two uncoupled cells immersed in the same amount of FGF (0.25 nM), with $f_2 \neq 1$, exhibit very different dynamics (Fig. 5a). The effect of coupling the cells is readily observed by comparing Fig. 5a,b,c. Before the coupling process, the two-cell system (with parameter f_2 set to 0.7) is characterized by a complex curve in the space defined by the calcium concentration in cell 2 vs. the calcium concentration in cell 1 (Fig. 5a). The form of this curve is characteristic of the dynamics of two independent cells. In Fig. 5b,c, we show the same plot of Fig. 5a for different coupling parameters after a transient. The transformation to a simple closed curve is indicative of a phase-locking process. After the coupling, the differences between the calcium concentrations of both cells diminish, as can be observed from the approach to a straight line of slope = 1 (Fig. 5b,c). However, a collapse to a straight line of slope = 1 is ruled out because of the cell's structural differences specified in the model by the number of IP_3 receptors.

When $f_2=0.5$, the interacting dynamics produc-

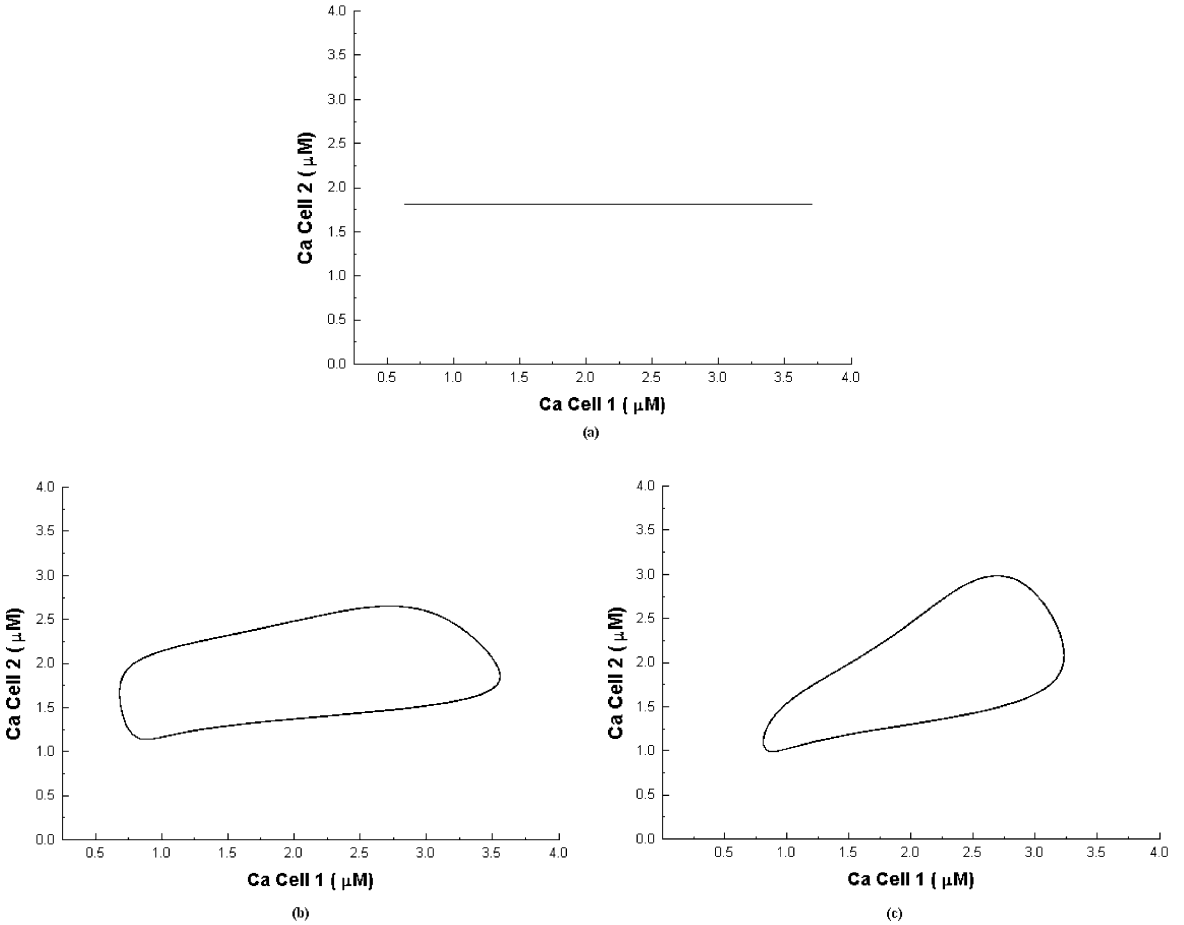

Fig. 6. Phase space plot for the calcium dynamics of: (a) two uncoupled cells; (b) soft coupling, $D_{Ca}=0.005\ s^{-1}$; and (c) strong coupling, $D_{Ca}=0.015\ s^{-1}$. In all panels, both cells were subjected to 0.25 nM of FGF. The parameters values used were: $f_2=0.5$ and $k_{18}^1=20\ \mu M^{-1}\ s^{-1}$.

es oscillatory entrainment. For this case, the dynamics of two uncoupled cells gives the straight line with zero slope shown in Fig. 6a. In the presence of weak coupling, this straight line changes into a closed curve with a limit cycle behavior (Fig. 6b). This curve narrows as the coupling coefficient is increased, settling at the coupling corresponding to Fig. 6c.

Although the mesodermal induction process is a collective one [32], the two-cell model can contribute to our understanding of how the calcium signal evoked by FGF can synchronize the temporal behavior of the signal carried by the MAPK cascade in cells with different structural properties.

If the Xbra transcription machinery is sensitive to either the amplitude or frequency of the MAPK cascade oscillations induced by calcium, then the intercellular calcium transport would modulate the expression of this gene [31]. This modulation process could be positive or negative under different circumstances [34].

For example, the coupling of the cells can induce oscillations in the Raf^* levels. This is shown in Fig. 7a,b, where, for $f_2=0.5$, cell 1 induces oscillations in the Raf^* level of the originally quiescent cell 2. These periodic variations in Raf^* activity are phase-locked to the periodic changes in the calcium level of each cell. In this

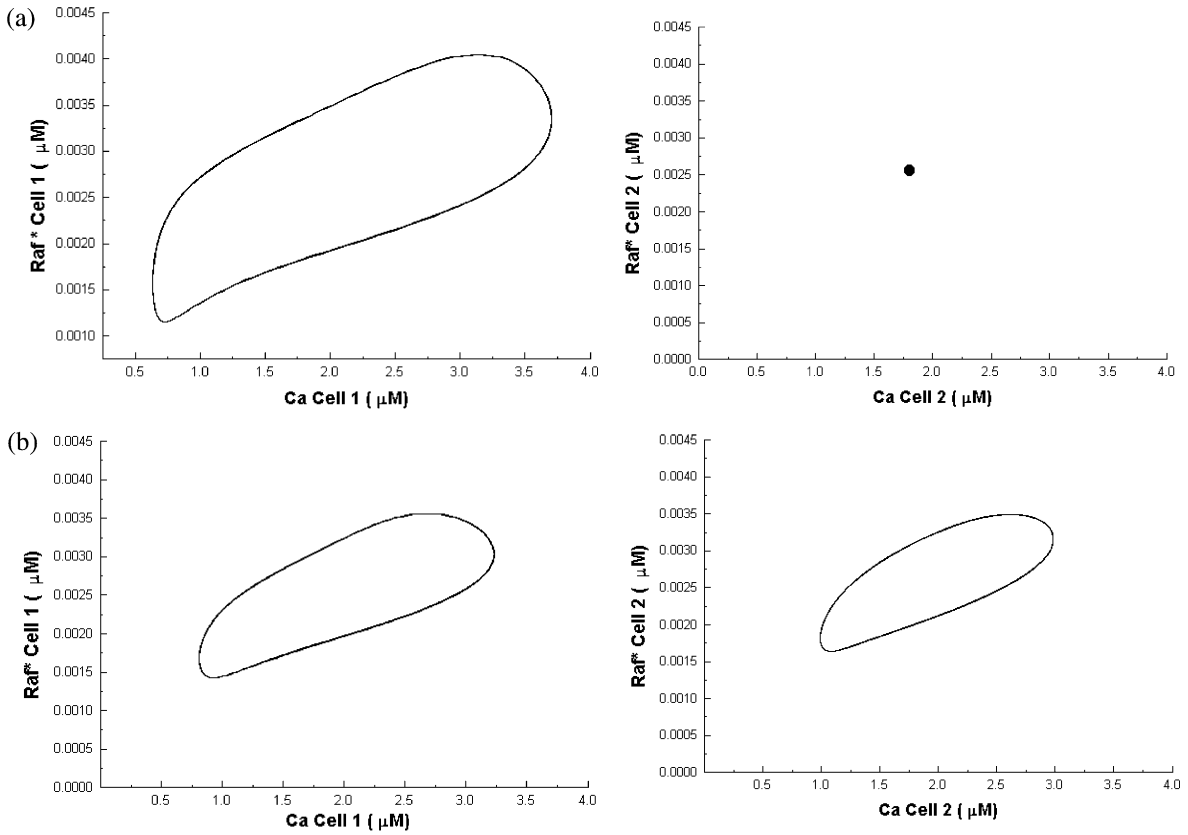

Fig. 7. Raf* vs. calcium phase space of the two-cell system immersed in 0.25 nM of FGF. (a) Uncoupled cells with $f_2=0.5$; (b) coupled cells with $f_2=0.5$. In panel (b) the parameter D_{Ca} is set to 0.015 s^{-1}. The parameter k_{18}^1 is set to 20 $\mu M^{-1}\ s^{-1}$ in all panels.

case the oscillatory behavior of the cell 2 Raf^* level tends to be less intense (Fig. 7b) than that of the triggering cell 1.

When two cells have an initially intrinsic oscillatory behavior, the coupling tends to synchronize them (Fig. 8a,b). However, differences persist due to the different number of IP_3 receptors.

4. Discussion

Each blastomere of the *Xenopus* embryo is a complex system, in which the signals from different parts of the embryo determine its fate. This fate depends on the cell's spatial localization and on its competence to respond to these signals. The response is mediated by intracellular signaling systems, which carry these signals to the nucleus and induce very specific genetic processes [31]. In particular, the FGF signaling system plays a central role during the mesodermal induction of the blastomeres of the equatorial zone of the embryo.

Our model attempts to clarify this role and takes into account the temporal behavior of the interaction of the IP_3–Ca^{2+} and MAPK signaling pathways associated with FGF. We assume that the temporal behavior of each pathway is essentially determined by its feedback loops, and that the concentrations of the other components of the pathway are in a quasi-steady state with respect to PLC^* and Raf^* concentrations. This approach allows us to model this complex system with a set of five non-linear differential equations that reflect the main qualitative features of the system.

In the model, the sources of the calcium spikes are the interactions of the cytoplasmic components of the Ca^{2+}-signaling system, rather than the

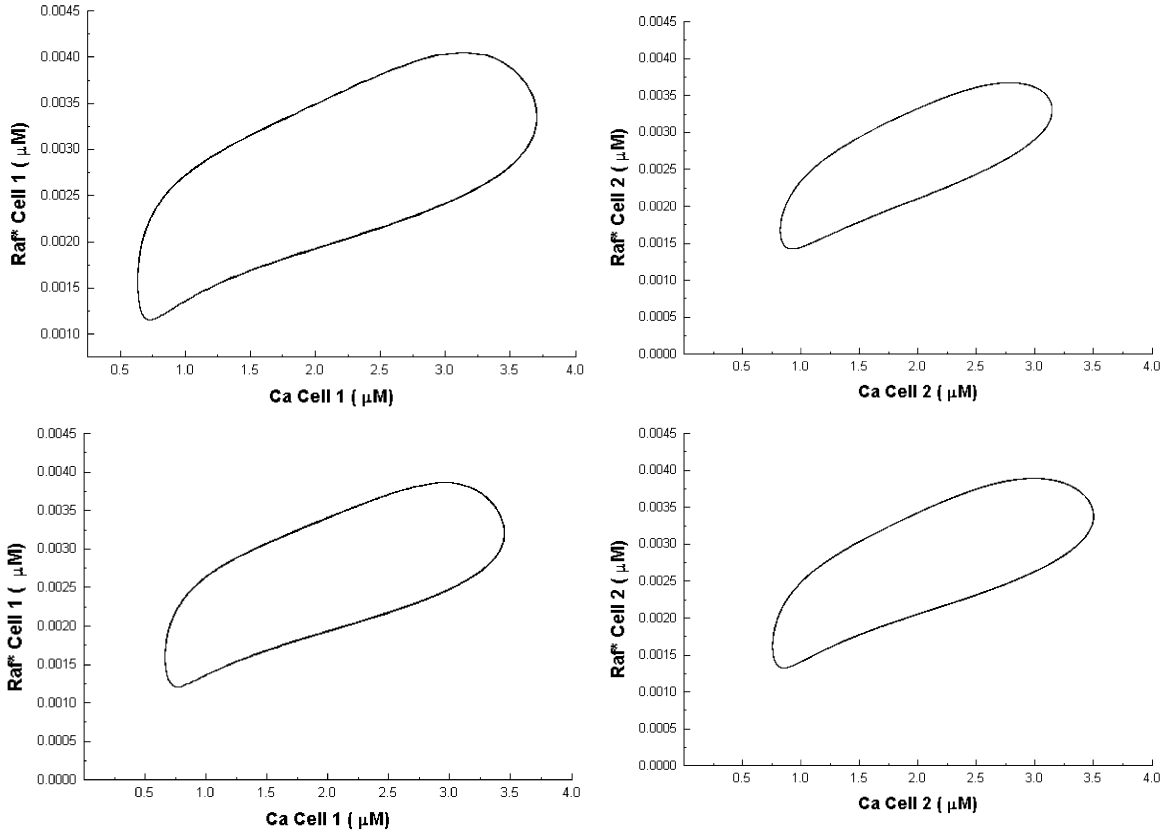

Fig. 8. Raf* vs. calcium phase space of the two-cell system immersed in 0.25 nM of FGF. (a) Uncoupled cells with $f_2=0.7$; (b) coupled cells with $f_2=0.7$. In panel (b) the parameter D_{Ca} is set to 0.015 s^{-1}. The parameter k_{18}^1 is set to 20 $\mu M^{-1}\ s^{-1}$ in all panels.

kinetics of the IP_3 receptor [23,36]. With this point of view, the positive feedback loop between Ca^{2+} and PLC is the main element for calcium spiking.

The link between this signaling system and the MAPK cascade is the activation of Raf by PKC^* (Fig. 1). The results from the numerical solutions of the model (Figs. 2 and 4) indicate that the calcium oscillatory signal induces a linear oscillatory response on the MAPK cascade, i.e. the output (Raf^* oscillations) has the same frequency as the input (Ca^{2+} spikes), but of different amplitude. This input and response relationship might be modified once the kinetics of the PKC translocation is taken into account.

The mRNA transcripts of PKC are located at the animal pole of the *Xenopus* oocyte [37] and this spatial localization is closely related to the great amount of IP_3R molecules found in the animal pole [11]. Thus, the animal pole is a rich calcium activity zone, while the vegetal pole seems to be less relevant to the embryo calcium-signaling activity. These structural and functional differences between both poles should have a meaning for the mesodermal induction process. The cells of the marginal zone of the embryo are subject to a set of inducting signals from the vegetal pole and the Nieuwkoop center, and to an intense periodic calcium signal from the animal pole [1]. Therefore, the link between the calcium and the MAPK systems may have a specific functional role at the animal pole, whereas they might be less important at the vegetal pole.

The MAPK cascade acts in a ‘switch-like’ relay system for the signal generated by the agonist input. The translocation of the activated MAPK to the nucleus can turn on the Xbra FGF-dependent

transcriptional machinery in a switch-like form [38]. This could be the basic response to the induction by FGF in the absence of interactions with other signaling pathways. This also could be the way in which the cells from the vegetal pole respond to FGF in the absence of the PKC link.

In the animal pole the scenario is very different, because the calcium spikes add an oscillatory component to the signal carried to the nucleus by the MAPK cascade. This new temporal property of the signal is meaningful only if the Xbra FGF-dependent transcription machinery is competent to respond to an oscillatory input [31]. This frequency response can be enhancing or inhibitory, depending on the amplitude, frequency and duration of the input signal [31,39].

Our model shows that cells with different number of IP_3R have different calcium dynamics, even when they are subject to the same agonist concentration, and that two cells with different calcium dynamics can be synchronized by the flux of this ion through the gap junctions. A cell without intrinsic calcium dynamics can acquire this feature when it contacts a cell with intense calcium spiking (Fig. 6).

These results from the model lead to a picture of the MBT embryo as a network of Ca^{2+} oscillators linked to a central pattern generator located at the prospective dorsal ectoderm domain over the A–V axis [1].

The consequence of this coupling over the Ca^{2+} dynamics of the embryo cells, as suggested by our model, is that the Xbra FGF-dependent transcription machinery of every cell is subject to the same frequency input, which means that the central pattern generator possibly induces an oscillatory signal that modulates the expression of the Xbra gene, although this signal is damped in some zones of the animal pole far from the generator [1].

Experimental data related to the frequency response of the Xbra FGF-dependent transcription machinery are not yet available. However, since all the cells of the marginal zone are apparently subject to the action of the same amount of FGF, an open possibility is that the oscillatory component of the FGF-MAPK signal may be linked to the ventralization of the mesoderm, counterbalancing the dorsalizing action of activin [3].

A possible hypothesis for the role of Ca^{2+} in the mesodermal induction process is that this signal periodically induces high levels of activation of the MAPK, which in turn can produce high levels of phosphorylated Smads 2 and 3. The phosphorylation of these Smads inhibits the dorsalizing signal from the activin pathway [40], while the periodic translocation of a high number of activated MAPK molecules into the nucleus can increase the activity of the of the FGF-dependent Xbra transcription machinery, enhancing the ventral features of the mesoderm. Finally, the calcium signal can also increase the level of activity of other molecules, such as the calmodulin and the gsk3 [41], in the zone near the central pattern generator. The activated calmodulin and gsk3 molecules can then also act as inhibitors of the dorsalizing signals [3,40] from the vegetal pole and the Nieuwkoop center, allowing an appropriate environment for the FGF-dependent expression of the Xbra and related genes.

Acknowledgments

José Díaz and Gerold Baier thank CONACyT for financial support, Gustavo Martínez-Mekler also acknowledges CONACyT under contract G34524-E. We also thank Germinal Cocho for interesting discussions.

References

[1] C. Leclerc, S.E. Webb, C. Daguzan, M. Moreau, A.L. Miller, Imaging patterns of calcium transients during neural induction in *Xenopus laevis* embryos, J. Cell. Sci. 113 (2000) 3519–3529.

[2] C. LaBonne, M. Whitman, Localization of MAP kinase activity in early *Xenopus* embryos: implications for endogenous FGF signaling, Dev. Biol. 183 (1997) 9–20.

[3] R. Harland, J. Gerhart, Formation and function of Spenmann's organizer, Annu. Rev. Cell. Dev. Biol. 13 (1997) 611–667.

[4] J.M.W. Slack, The first pure embryonic inducing factor, BioEssays 21 (1999) 525–532.

[5] P.J. Ryan, G.D. Paterno, L.L. Gillespie, Identification of phosphorylated proteins associated with the fibroblast growth factor receptor type I during early *Xenopus* development, Biochem. Biophys. Res. Commun. 244 (1998) 763–767.

[6] P.J. Ryan, L.L. Gillespie, Phosphorylation of phospholipase Cγ1 and its association with the FGF receptor is developmentally regulated and occurs during mesoderm induction in *Xenopus laevis*, Dev. Biol. 166 (1994) 101–111.
[7] B. Christen, J.M.W. Slack, Spatial response to fibroblast growth factor signalling in *Xenopus* embryos, Development 126 (1999) 119–125.
[8] E.S. Casey, M.A. O'Reilly, F.L. Conlon, J.C. Smith, The T-box transcription factor Brachyury regulates expression of eFGF through binding to a non-palindromic response element, Development 125 (1998) 3887–3894.
[9] A.J. Muslin, K.G. Peters, L.T. Williams, Direct activation of phopholipase C-γ by fibroblast growth factor receptor is not required for mesoderm induction in *Xenopus* animal caps, Mol. Cell Biol. 14 (1994) 3006–3012.
[10] S. Kume, Role of the inositol 1,4,5-trisphosphate receptor in early embryonic development, Cell. Mol. Life Sci. 56 (1999) 296–304.
[11] S. Kume, A. Muto, H. Okano, K. Mikoshiba, Developmental expression of the inositol 1,4,5-trisphosphate receptor and localization of inositol 1,4,5-trisphosphate during early embryogenesis in *Xenopus laevis*, Mech. Dev. 66 (1997) 157–168.
[12] R. Carballada, H. Yasuo, P. Lemaire, Phosphatidylinositol-3 kinase acts in parallel to the ERK MAP kinase in the FGF pathway during *Xenopus* mesoderm induction, Development 128 (2001) 35–44.
[13] E. Browaeys-Poly, K. Cailliau, J. Vilain, Signal transduction pathways triggered by fibroblast growth factor receptor 1 expressed in *Xenopus laevis* oocytes after fibroblast growth factor 1 addition. Role of Grb2, phosphatidylinositol 3-kinase, Scr tyrosine kinase, and phospholipase Cγ, Eur. J. Biochem. 267 (2000) 6256–6263.
[14] M.A. Nugent, E.R. Edelman, Kinetics of basic fibroblast growth factor binding to its receptor and heparan sulfate proteoglycan: a mechanism for co-operativity, Biochemistry 31 (1992) 8876–8883.
[15] P. Klint, L. Claesson-Welsh, Signal transduction by fibroblast growth factor receptor, Front. Biosci. 4 (1999) 165–177.
[16] L. Pellegrini, D.F. Burke, F. von Delft, B. Mulloy, T.L. Blundell, Crystal structure of fibroblast growth factor receptor ectodomain bound to ligand and heparin, Nature 407 (2000) 1029–1034.
[17] M. Fannon, K.E. Forsten, M.A. Nugent, Potentiation and inhibition of bFGF binding by heparin: a model for regulation of cellular response, Biochemistry 39 (2000) 1434–1445.
[18] G. Karp, Cell and Molecular Biology, Wiley, New York, 1999.
[19] B.N. Kholodenko, Negative feedback and ultrasensitivity can bring about oscillations in the mitogen-activated protein kinase cascades, Eur. J. Biochem. 267 (2000) 1583–1588.
[20] B.N. Kholodenko, O.V. Demin, G. Moehren, J.B. Hoek, Quantification of short-term signaling by epidermal growth factor receptor, J. Biol. Chem. 274 (1999) 30169–30181.
[21] M.A. Rizzo, K. Shome, S.C. Watkins, G. Romero, The recruitment of Raf-1 to membranes is mediated by direct interaction with phosphatidic acid and is independent of association with Ras, J. Biol. Chem. 275 (2000) 23911–23918.
[22] T.P. Garrington, G.L. Johnson, Organization and regulation of mitogen-activated protein kinase signalling pathways, Curr. Opin. Cell. Biol. 11 (1999) 211–218.
[23] U. Kummer, L.F. Olsen, C.J. Dixon, A.K. Green, E. Bornberg-Bauer, G. Baier, Switching from simple to complex oscillations in calcium signalling, Biophys. J. 79 (2000) 1188–1195.
[24] D.K. Morrison, R.E. Cutler, The complexity of Raf-1 regulation, Curr. Opin. Cell Biol. 9 (1997) 174–179.
[25] T. Meyer, L. Stryer, Calcium spiking, Annu. Rev. Biophys. Chem. 20 (1991) 153–174.
[26] M.J. Rebecchi, S.N. Pentyala, Structure, function and control of phosphoinositide-specific phospholipase C, Physiol. Rev. 80 (2000) 1291–1335.
[27] S. Kume, T. Inoue, K. Mikoshiba, Gαs family G proteins activate IP3-Ca^{2+} signaling via Gβγ and transduce ventralizing signals in *Xenopus*, Dev. Biol. 226 (2000) 88–103.
[28] F. Hofmann, I. Lacinová, N. Klugbauer, Voltage-dependent calcium channels: from structure to function, Rev. Physiol. Biochem. Pharmacol. 139 (1999) 33–87.
[29] A.P. LeBeau, D.I. Yule, G.E. Groblewski, J. Sneyd, Agonist-dependent phosphorylation of the inositol 1,4,5-trisphosphate receptor: a possible mechanism for agonist-specific calcium oscillations in pancreatic acinar cell, J. Gen. Physiol. 113 (1999) 851–871.
[30] I. Bezprozvanny, J. Watras, B.E. Erlich, Bell-shaped calcium-response curves of Ins(1,4,5)P3 and calcium-gated channels from endoplasmic reticulum of cerebellum, Nature 351 (1991) 751–754.
[31] M.J. Berridge, The AM and FM of calcium signalling, Nature 386 (1997) 759–760.
[32] L. Wolpert, R. Beddington, J. Brockers, T. Jesell, P. Lawrence, E. Megerowitz, Principles of Development, Oxford University Press, Oxford, 1998.
[33] J.M.W. Slack, Essential Developmental Biology, Blackwell, Oxford, 2001.
[34] K.L. Curran, R.M. Grainger, Expression of activated MAP kinase in *Xenopus laevis* embryos: evaluating the roles of FGF and other signalling pathways in early induction and patterning, Dev. Biol. 228 (2000) 41–56.
[35] J.A. Rottingen, J.G. Iversen, Ruled by waves? Intracellular and intercellular calcium signaling, Acta Physiol. Scand. 169 (2000) (2000) 203–219.
[36] J. Keener, J. Sneyd, Mathematical Physiology, Springer-Verlag, New York, 1998.

[37] A. Bashirullah, R.L. Cooperstok, H.D. Lipshitz, RNA localization in development, Annu. Rev. Biochem. 67 (1998) 335–394.
[38] C.F. Huang, J.E. Ferrell, Ultrasensitivity in the mitogen-activated protein kinase cascade, Proc. Natl. Acad. Sci. USA 93 (1996) 10078–10083.
[39] C.J. Marshall, Specifity of receptor tyrosine kinase signaling: transient versus sustained extracellular signal-regulated kinase activation, Cell 20 (1995) 179–185.
[40] S.A. Pangas, T.K. Woodruff, Activin signal transduction pathways, Trends Endocrinol. Metab. 11 (2000) 309–314.
[41] J.A. Hartigan, G.V.W. Johnson, Transient increases in intracellular calcium result in prolonged site-selective increase in Tau phosphorylation through a glycogen synthase kinase 3β-dependent pathway, J. Biol. Chem. 274 (1999) 21395–21401.